



14th International Conference on Medical Image Computing and Computer Assisted Intervention

# Manifold embedding for modeling spinal deformations

Samuel Kadoury

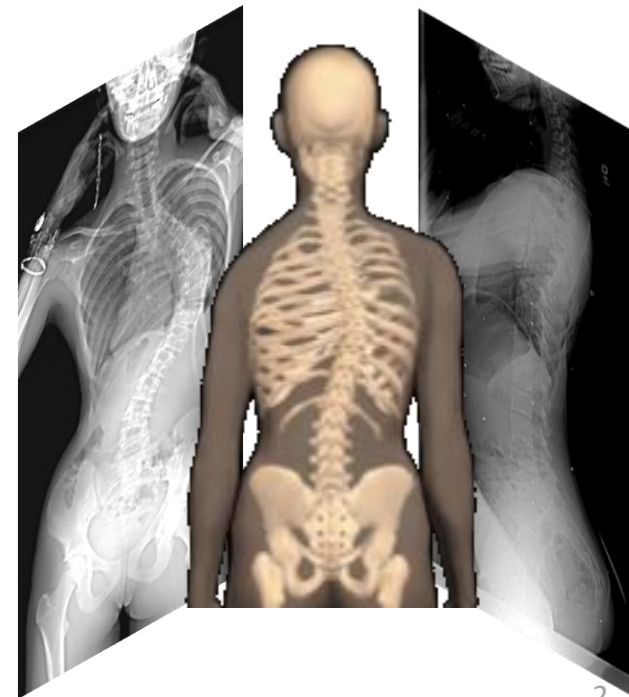
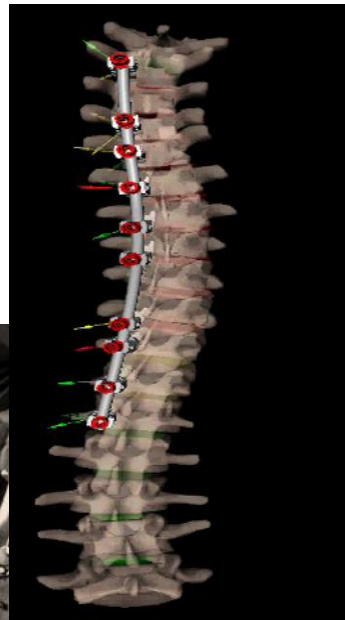
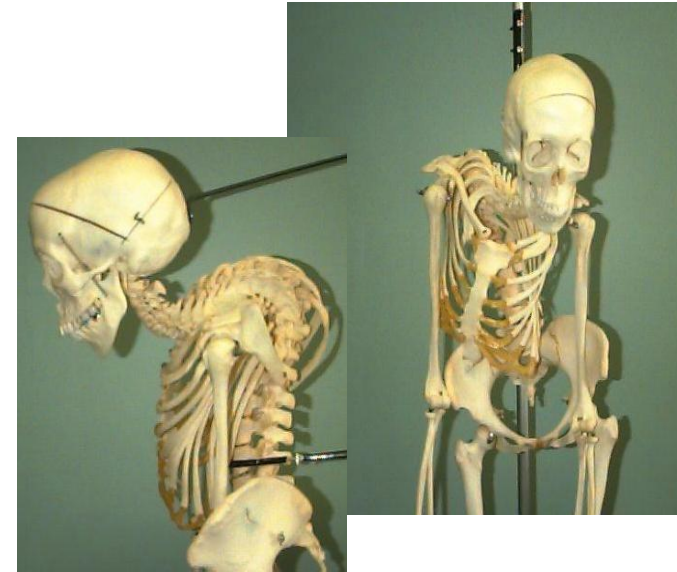
Philips Research North America

MICCAI 2011 Tutorial on Manifold Learning with Medical Images  
September 22<sup>th</sup>, 2011



# Spinal deformities

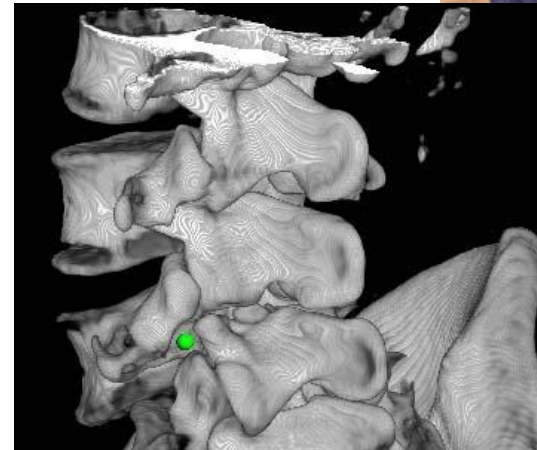
- **Adolescent Idiopathic Scoliosis (AIS):**
  - Complex and progressive 3D deformation of the musculoskeletal trunk
  - Radiographic imaging is the most frequently used modality to evaluate the pathology
  - Volumetric imaging modalities remains **limited** (radiation dosage, posture)
- **Surgical correction**



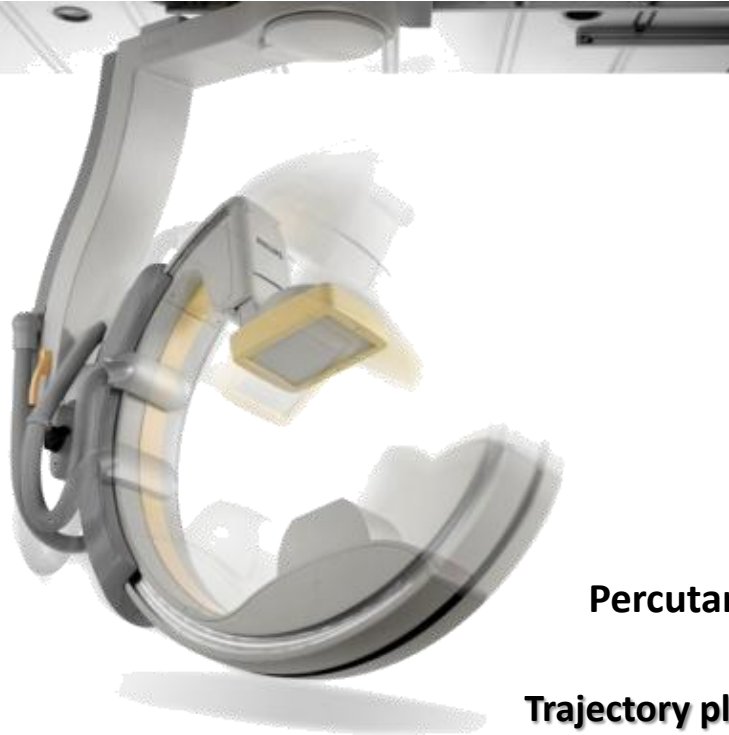
# Interventional X-ray & CBCT



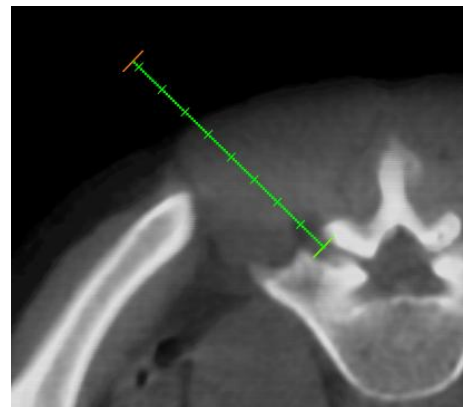
CBCT acquisition



Percutaneous vertebroplasties (nerves, vertebral articulations)



Trajectory planning



Fluoro image guidance

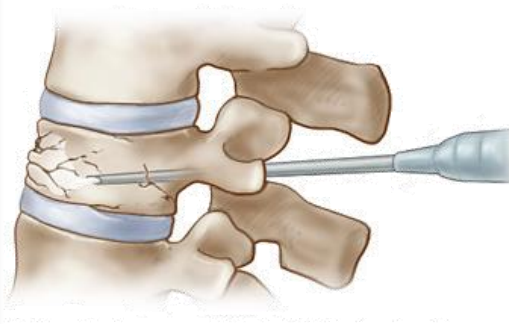
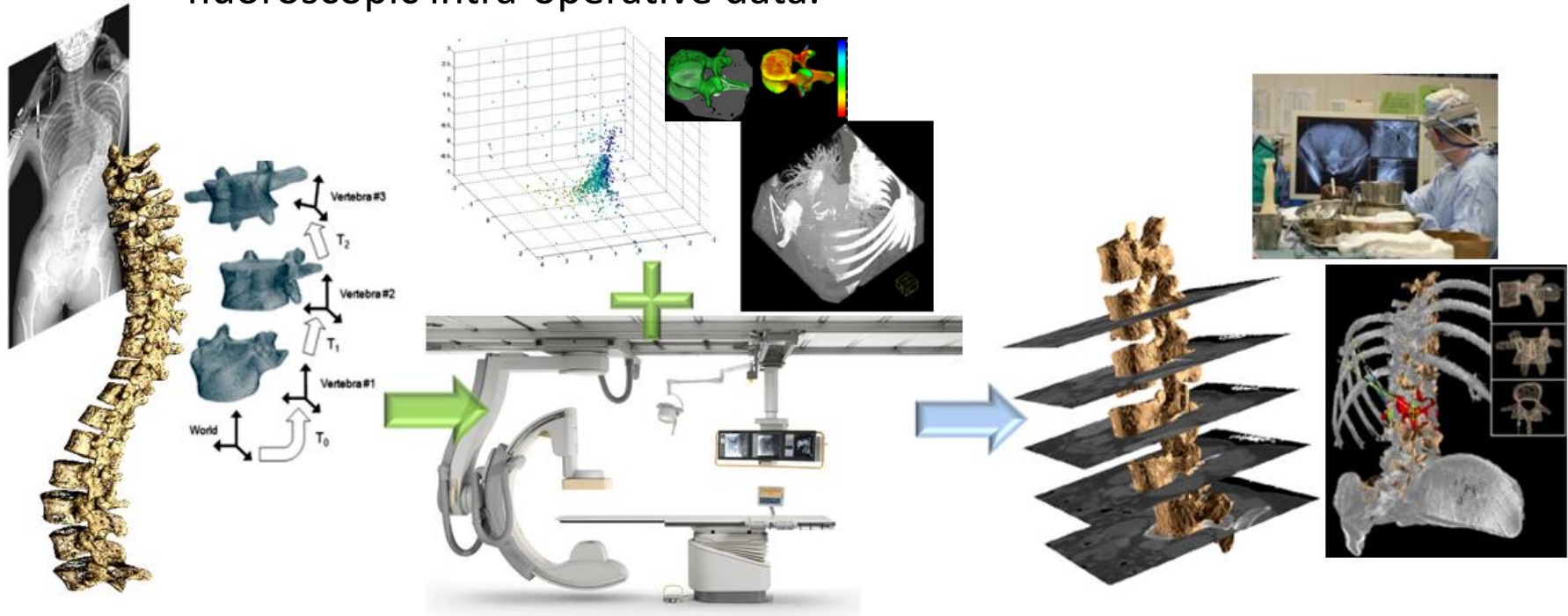


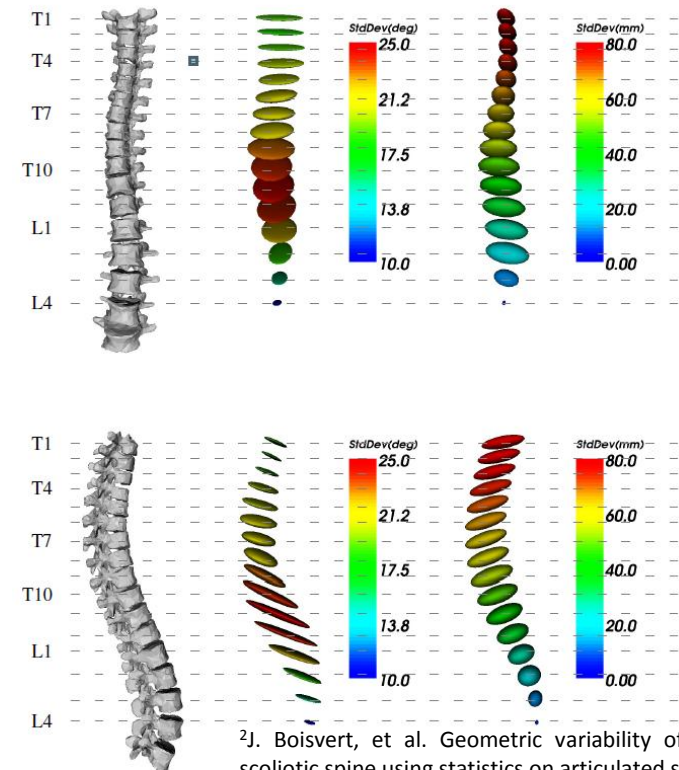
# Image-guided spinal surgery

- Interventional operating room
  - Fusion of pre-operative biplane model with CBCT images based on articulated deformation using MRFs.
  - Real-time inference of annotated geometrical spine model to tracked fluoroscopic intra-operative data.

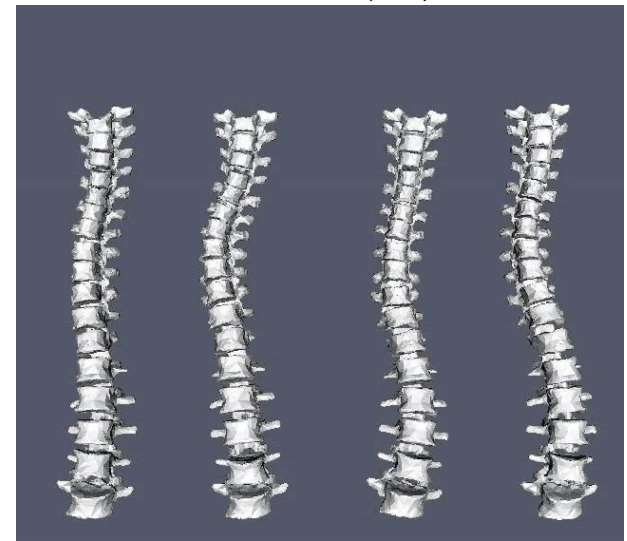


# Variability in spine deformation

- High variability of the spine's natural curvature and complex nonlinear structure.
- Use of linear statistics (PCA) are inapplicable to model such articulated structures for diagnostic or intra-operative imaging purposes.
- To overcome these challenges, an alternative approach maps the high-dimensional observation data (3D spine population) that are presumed to lie on a nonlinear manifold.



<sup>2</sup>J. Boisvert, et al. Geometric variability of the scoliotic spine using statistics on articulated shape models. *IEEE TMI* (2008).

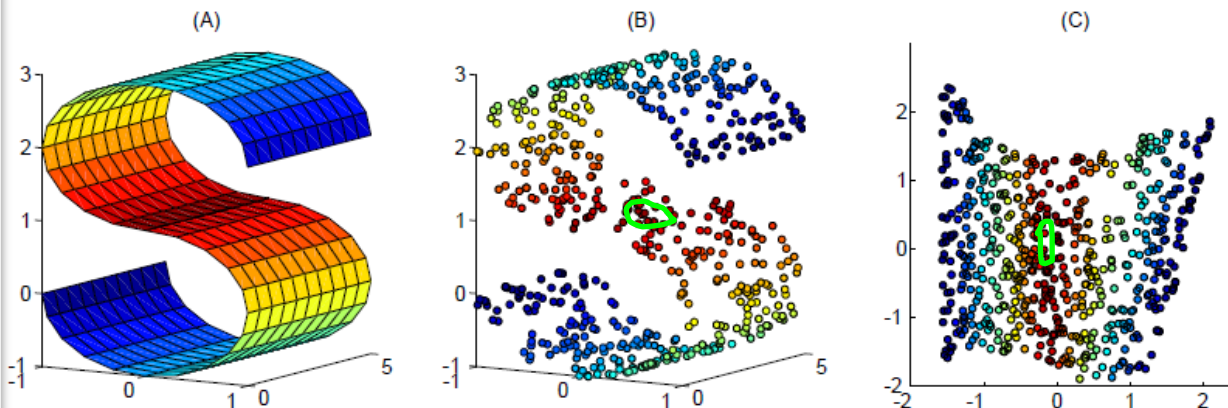


# Outline

- **Background on Locally Linear Embedding (LLE)**
  - Data representation
  - Neighbourhood selection
  - Creating the manifold embedding
- **Pre-operative reconstruction of an articulated 3D spine**
  - Model initialization
  - Regression functions for inverse mapping
- **Pathology classification from the low-dimensional manifold**
- **Inference of the intra-operative spine geometry from CT**
  - Manifold-based constraints ensuring geometrical consistency
  - Optimization of manifold parameters for direct model representation

# Locally Linear Embedding

- Nonlinear dimensionality reduction technique proposed by S. Roweis and L. Saul (Science, 2000) for exploratory data analysis and visualization<sup>3</sup>.
- Analyze large amounts of multivariate data in order to discover a compact representation of the high-dimensional data.
- Unsupervised learning algorithm that computes low-dimensional, neighborhood-preserving embeddings of high-dimensional inputs.
- LLE is able to learn the global structure of nonlinear manifolds, revealing the underlying distribution of the data which can be used for statistical modeling.

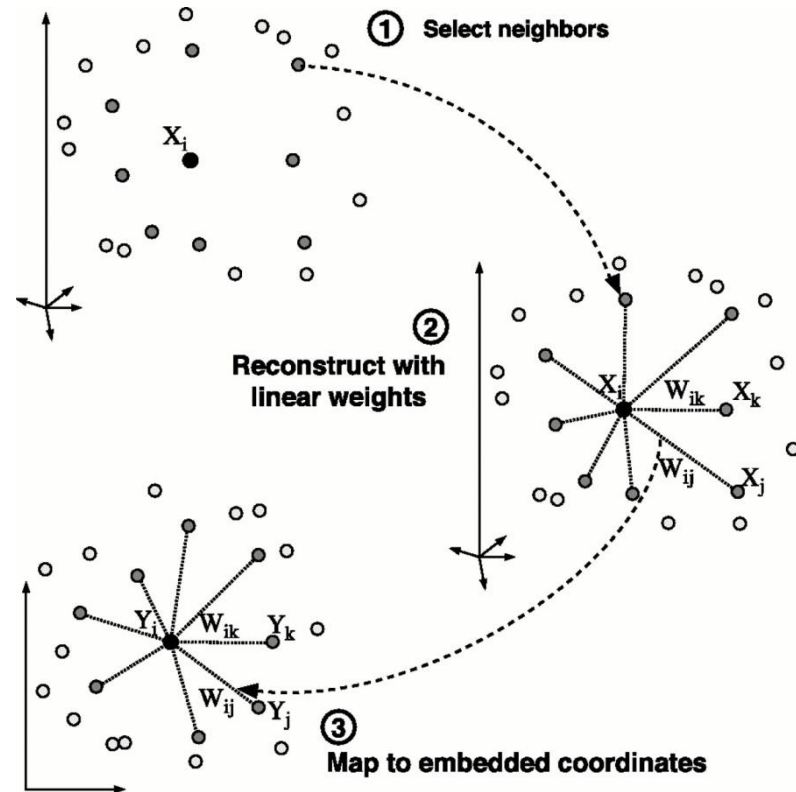


<sup>3</sup>S. Roweis and L. Saul. Nonlinear Dimensionality Reduction by Locally Linear Embedding. *Science* 22 December 2000: pp. 2323-2326

# Locally Linear Embedding

- Data consisting of  $N$  real-valued observation vectors  $X_i$ , each of high dimensionality  $D$ , sampled from some underlying manifold.
- Each data point and its neighbors assumed to lie on or close to a locally linear patch of the manifold.
- In its simplest form, LLE identifies the  $K$  nearest neighbors per data point, as measured by Euclidean distance.
- Local geometry of these patches by linear coefficients that reconstruct each data point from its neighbors. Reconstruction errors are measured by the cost function:

$$\mathcal{E}(W) = \sum_{i=1}^N \left\| X_i - \sum_{j=1}^K W_{ij} X_{ij} \right\|^2$$

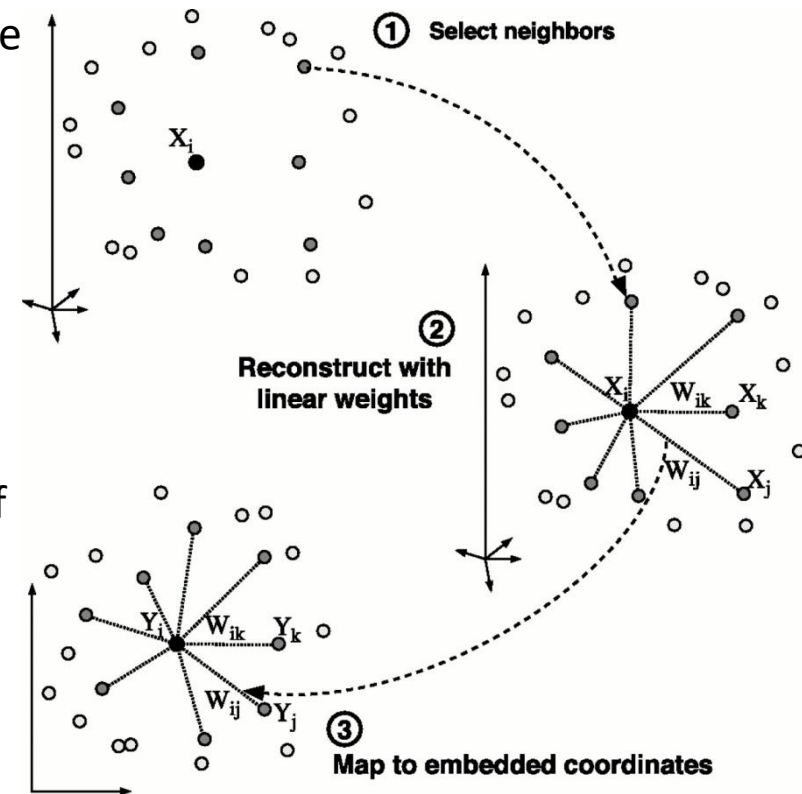


# Locally Linear Embedding

- Each high-dimensional observation  $X_i$  is mapped to a low-dimensional vector  $Y_i$  representing global internal coordinates on the manifold. This is done by choosing  $d$ -dimensional coordinates  $Y_i$  to minimize the embedding cost function:

$$\Phi(Y) = \sum_{i=1}^N \left\| Y_i - \sum_{j=1}^K W_{ij} Y_j \right\|^2$$

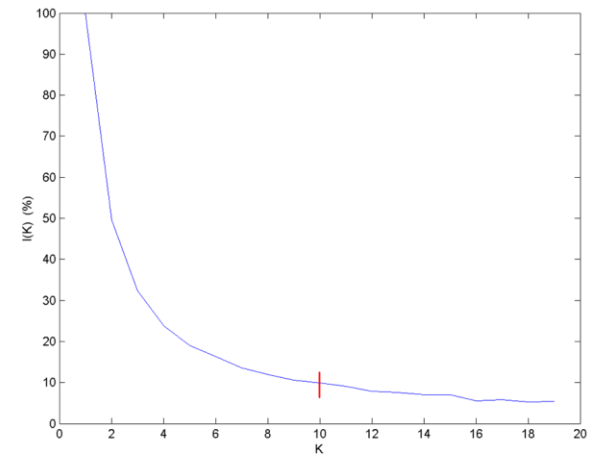
- Reconstruction weights  $W_{ij}$  reflect intrinsic geometric properties of the data that are invariant to the linear mapping — consisting of a translation, rotation, and rescaling.
- The same weights  $W_{ij}$  that reconstruct the  $i^{\text{th}}$  data point in  $D$  dimensions should also reconstruct its embedded manifold coordinates in  $d$  dimensions.



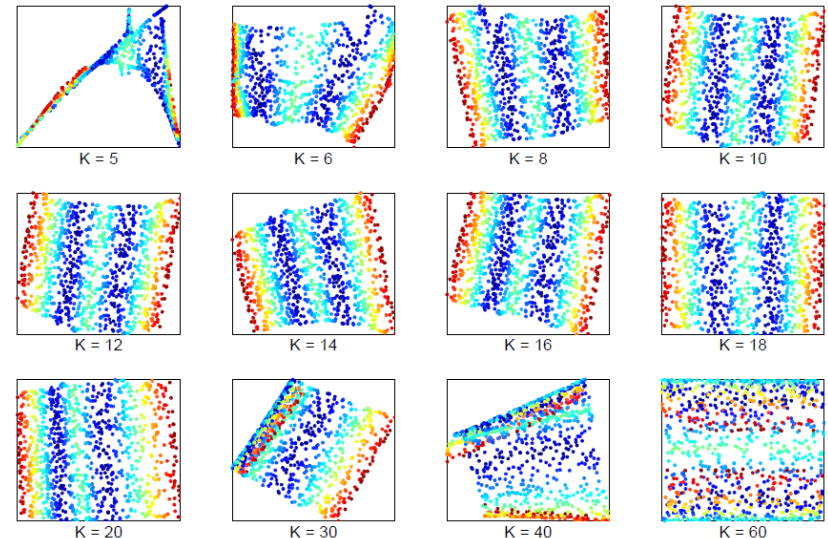
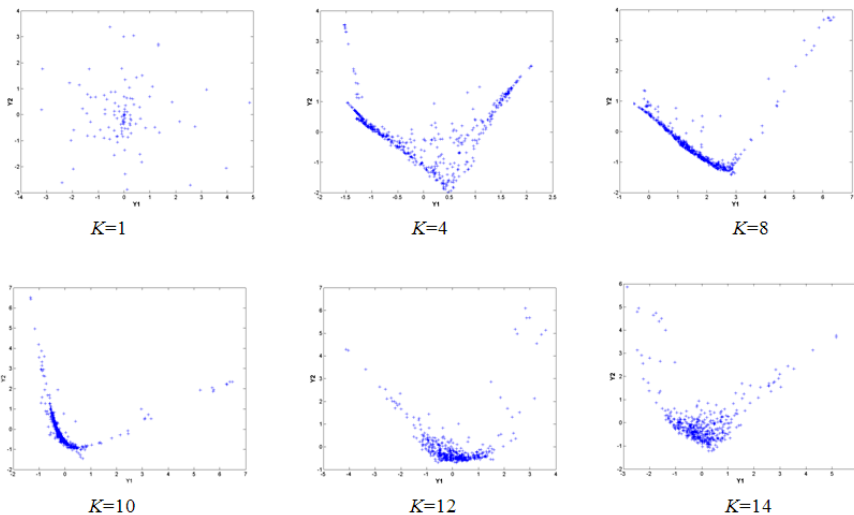
# Parameter selection

- Neighborhood size  $K$ :
  - Stability of the resulting embeddings determined from the increase in the number of significant weights  $W(K)$  [Kouropteva et al., 2003].
  - $K$  is large enough to capture most local contexts and the resulting embedding space is relatively stable using the increase in significant weights  $I(K)$ :

$$I(K) = \frac{W(K+1) - W(K)}{W(K)} \times 100$$

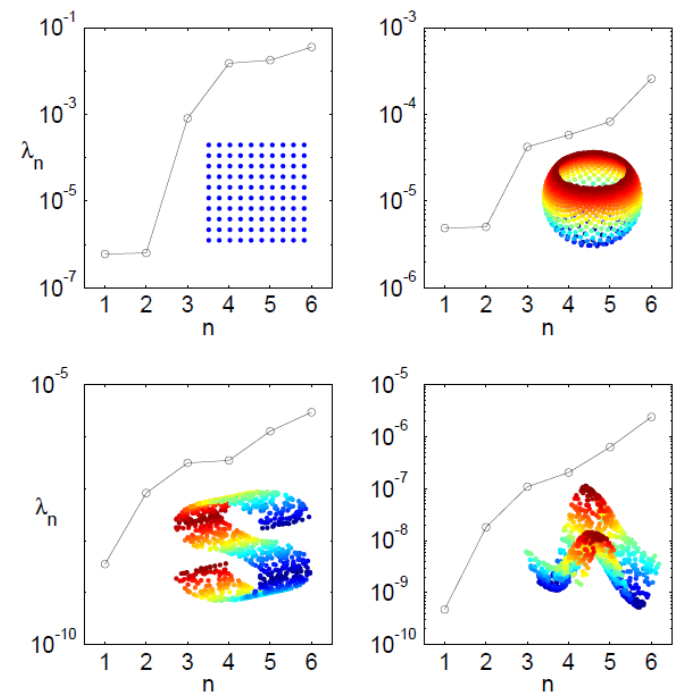
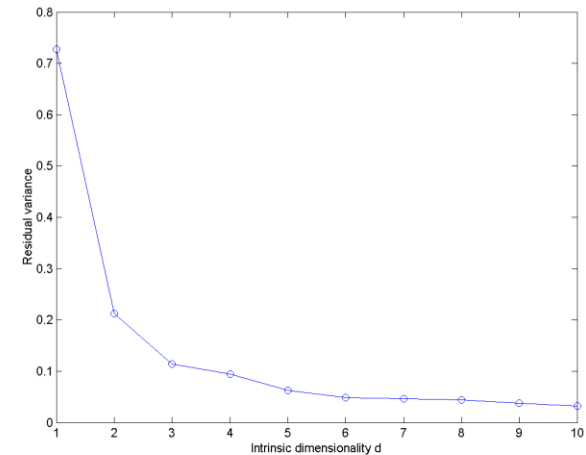


O. Kouropteva et al. Classification of Handwritten digits using supervised locally linear embedding algorithm and support vector machine. *Symp. on Artif. Neural Networks*, pp. 229-234, 2003.



# Parameter selection

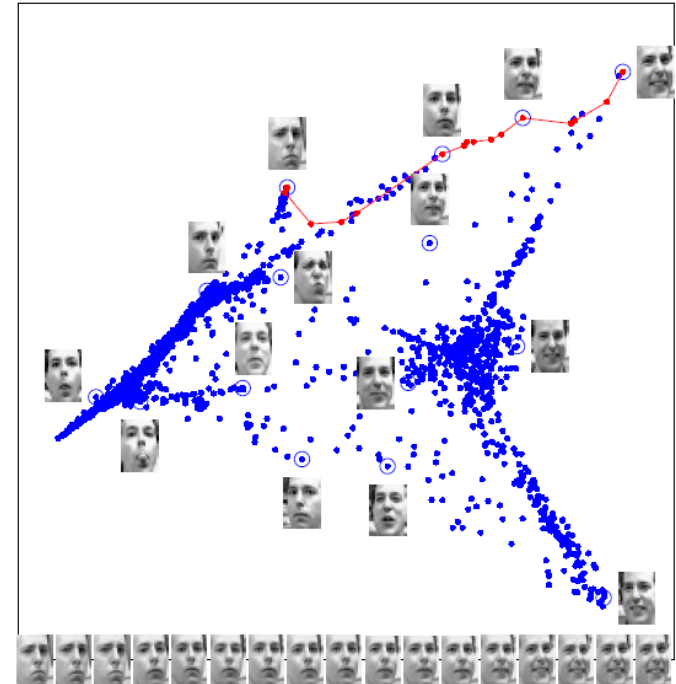
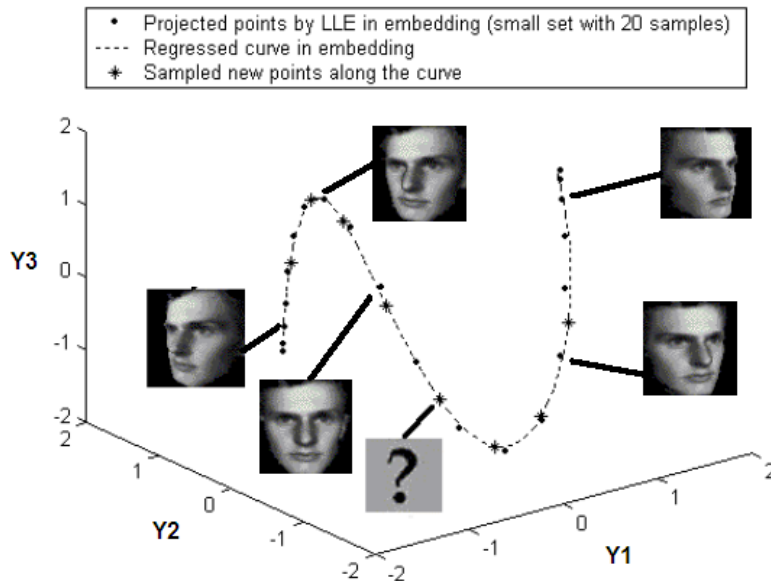
- Intrinsic dimensionality  $d$ :
  - Lowest residual variance  $\rho$  defined by the distance between pairs of data points can be used for this purpose [Ridder et al., 2002].
  - $\rho = 1 - r^2_{D_X D_Y}$ , where  $r^2_{D_X D_Y}$  is the standard linear correlation coefficient taken over all entries of  $D_X$  and  $D_Y$ .  $D_X$  and  $D_Y$  represent matrices of the Euclidean distances between pairs of points in  $X$  (input points in  $D$ -space) and  $Y$  (output points computed by LLE in  $d$ -space)
- Limited reliability of the number of eigenvalues that are appreciable in magnitude to the smallest nonzero eigenvalue of the cost matrix.



# Application to face recognition

Images of faces mapped into the embedding space ( $d=2$ ) demonstrating the variability in pose and expression.

L. Saul and S. Roweis, "Think globally, fit locally: unsupervised learning of non-linear manifolds", *TR MS CIS-02-18*, U. Penn, 2002.



Analytical representation of the manifold of high-dimensional data by learning the common information from high-density data to estimate unseen points in the manifold.

J. Wang, et al. "An Analytical Mapping for LLE and Its Application in Multi-Pose Face Synthesis", *14th BMVC.*, 2003.

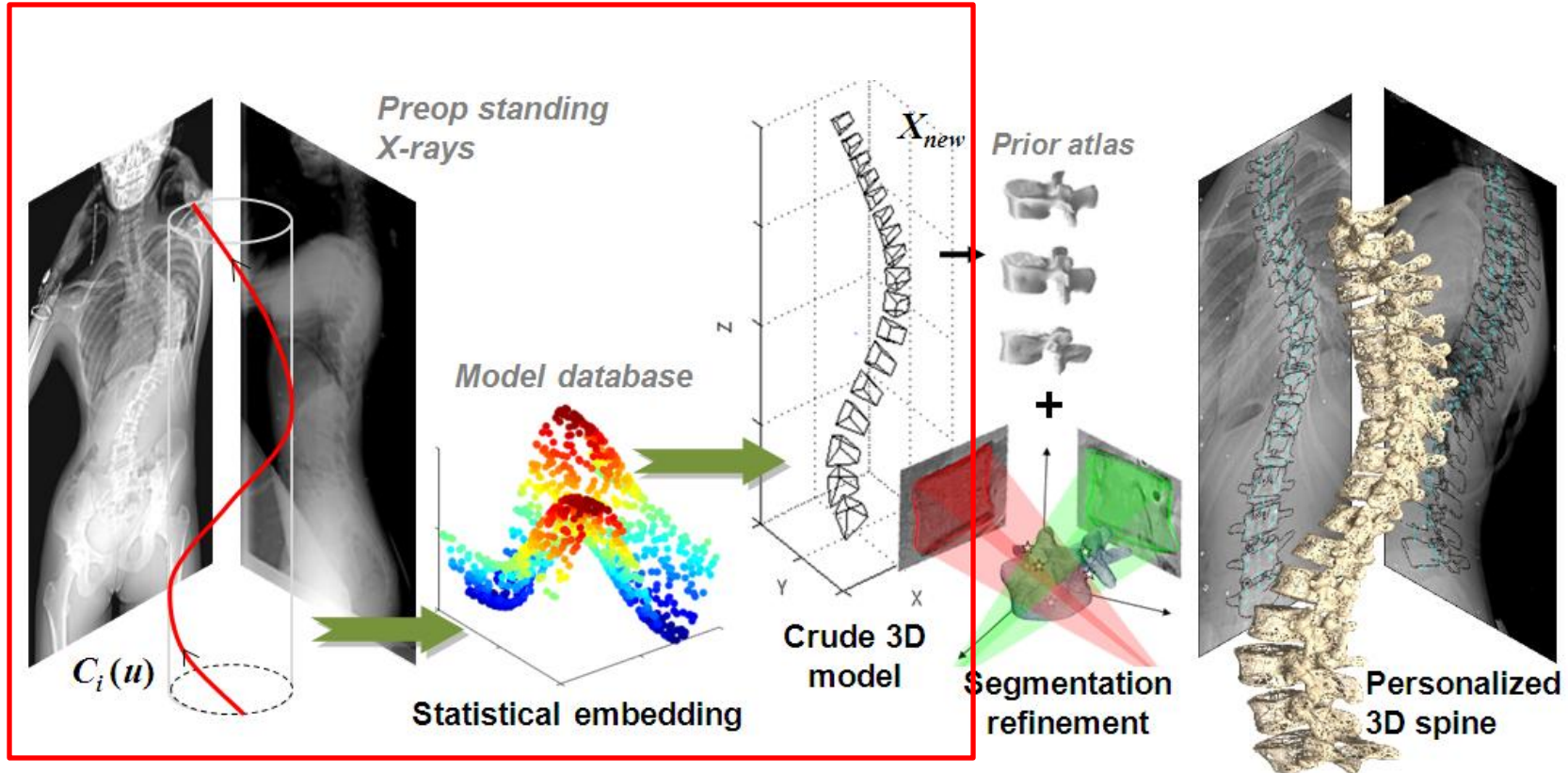
# Outline

- Background on Locally Linear Embedding (LLE)
  - Data representation
  - Neighbourhood selection
  - Creating the manifold embedding
- **Pre-operative reconstruction of an articulated 3D spine**
  - Model initialization
  - Regression functions for inverse mapping
- Pathology classification from the low-dimensional manifold
- Inference of the intra-operative spine geometry from CT
  - Manifold-based constraints ensuring geometrical consistency
  - Optimization of manifold parameters for direct model representation

# Pre-operative 3D reconstruction

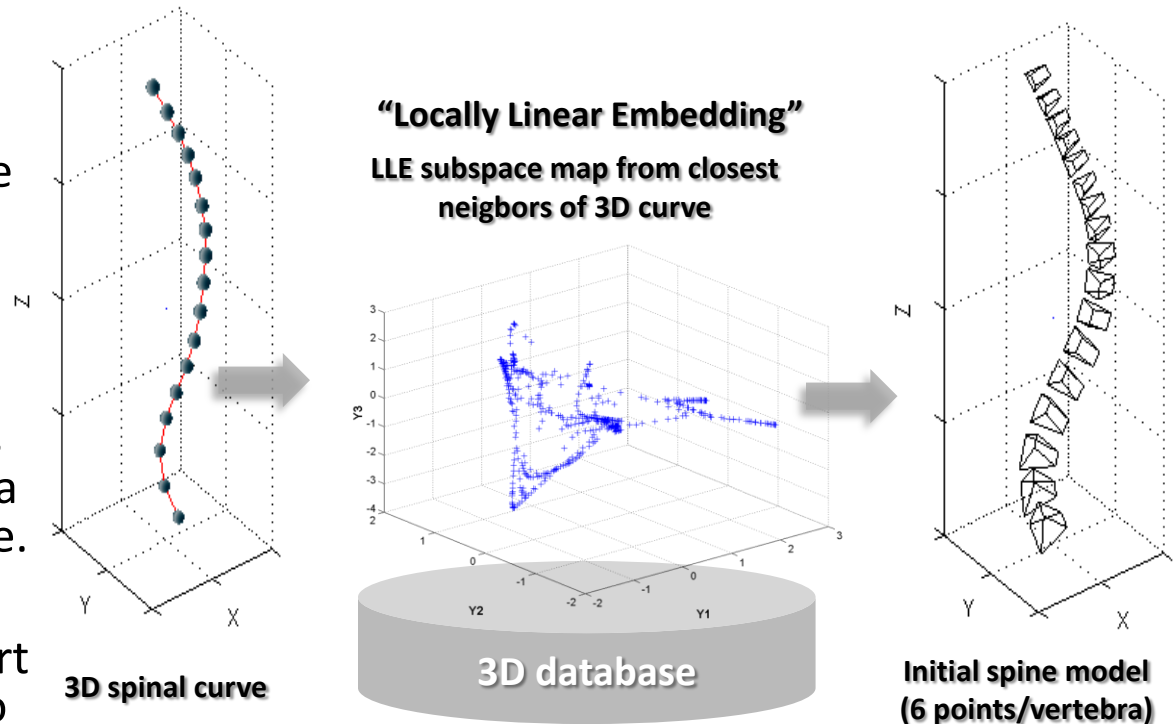
- Personalized 3D reconstruction of the pathological spine from diagnostic biplanar X-ray images

Kadoury et al., IEEE TMI (28), 2009.



# Statistical modeling of the spine

- Dimensionality reduction of the extracted spinal curve in the low-dimensional manifold embedding.
- Generates an approximate model from the closest neighbors in a 3D database containing 732 scoliotic models.
- Manifold establishes the patterns of legal variations of spine shape changes in a low-dimensional sub-space.
- Use of an analytical support vector regression model to accomplish the inverse mapping of a new manifold data point onto the high-dimensional space.



# Algorithm for generating approximate model

Given  $N$  spine models expressed by the B-splines  $C(u)_i$ ,  $C(u)_i \in R^D$ ,  $i \in [1, N]$ , each of dimensionality  $D$ , it provides  $N$  points  $Y_i$ ,  $Y_i \in R^d$ ,  $i \in [1, N]$  where  $d \ll D$ . The algorithm has four sequential steps:

- **Step 1.** Select the  $K$  closest neighbors for each point using the Frechet distance.
- **Step 2.** Solve the manifold reconstruction *weights*:

$$\varepsilon(W) = \sum_{i=1}^N \left\| C(u)_i - \sum_{j=1}^K W_{ij} C(u)_{ij} \right\|^2$$

where  $C(u)_i$  is a data vector and  $\varepsilon(W)$  sums the squared distances between all data points and their corresponding reconstructed points.

- **Step 3.** Map each high-dimensional  $C(u)_i$  to a low-dimensional  $Y_i$ , representing the global internal coordinates using a cost function which minimizes the reconstruction error :

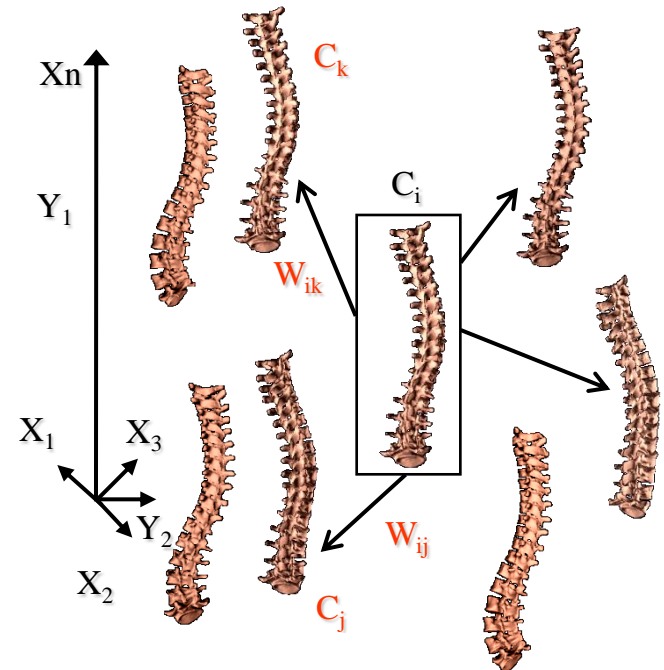
$$\Phi(Y) = \sum_{i=1}^N \left\| Y_i - \sum_{j=1}^K W_{ij} Y_{ij} \right\|^2$$

- **Step 4.** Apply an analytical method based on nonlinear regression to perform the inverse mapping from the  $d$  embedding :

$$X_{new} = F(Y_{new}) = [x_{new1}, \dots, x_{newD2}]^T = [f_1(Y_{new}), \dots, f_{D2}(Y_{new})]^T$$

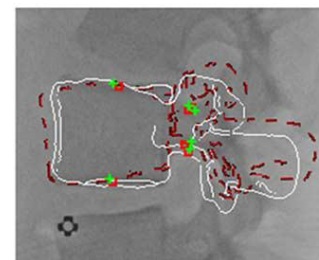
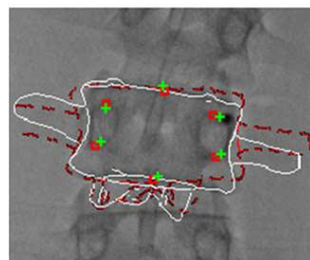
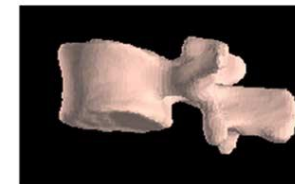
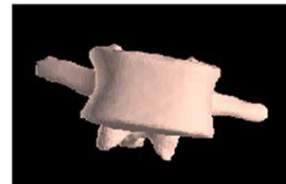
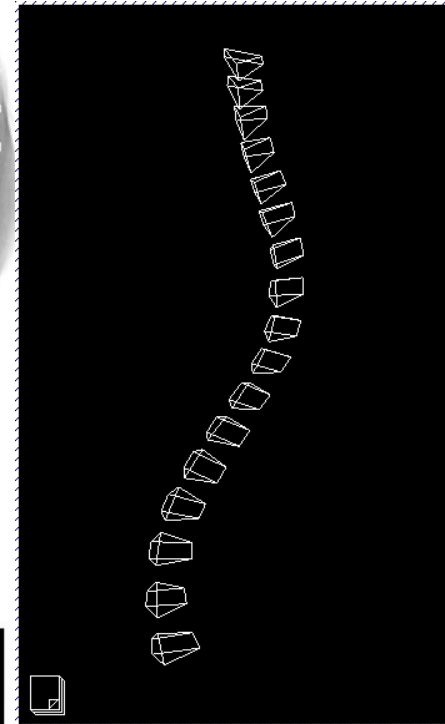
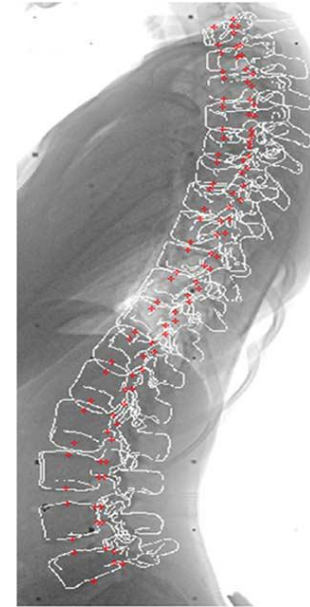
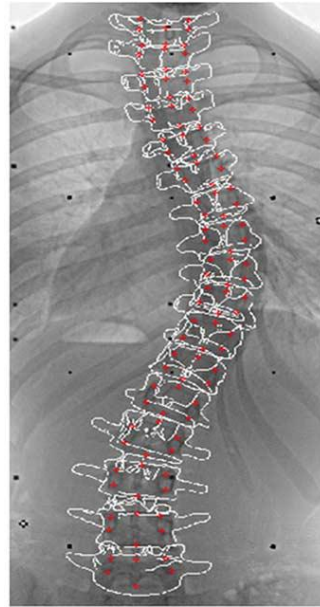
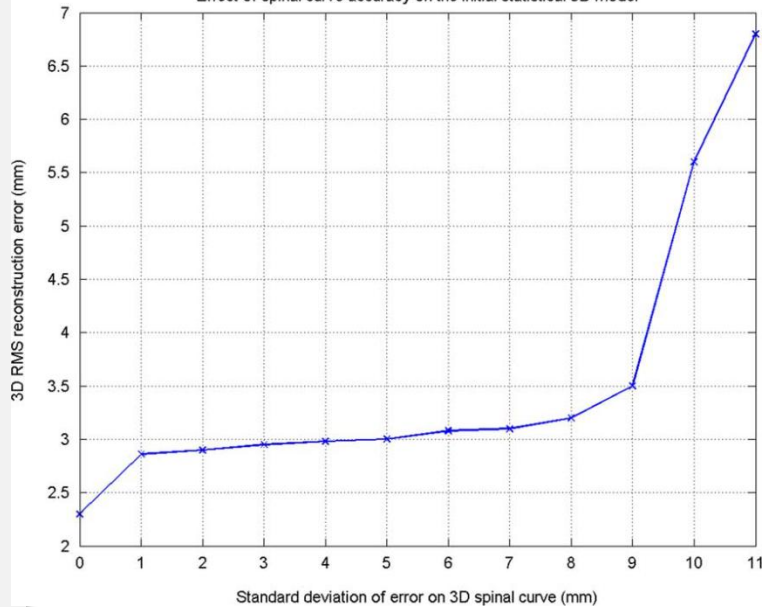
$x_i = f_i(Y) = \sum_j \alpha_{ij} k(Y, Y_j) + b$  is a SVR regression model using a RBF kernel  
 $X_{new} = (s_1, s_2, \dots, s_{17})$ , where  $s_i$  is a vertebra model defined by  $s_i = (p_1, p_2, \dots, p_6)$ , and  $p_i = (x_i, y_i, z_i)$  is a 3D vertebral landmark

Multidimensional distribution of scoliotic models



# Biplanar reconstruction results

Effect of spinal curve accuracy on the initial statistical 3D model

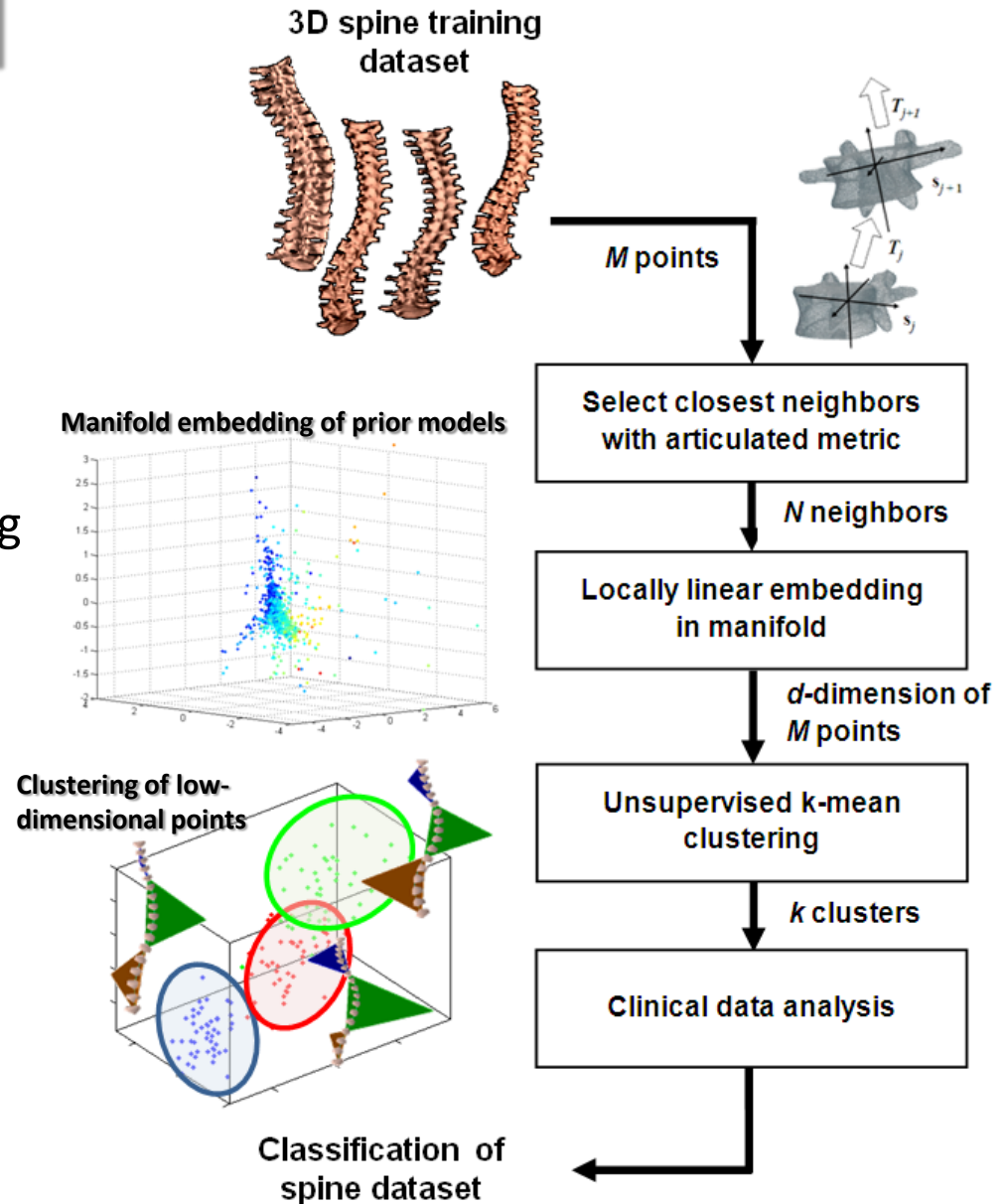


# Outline

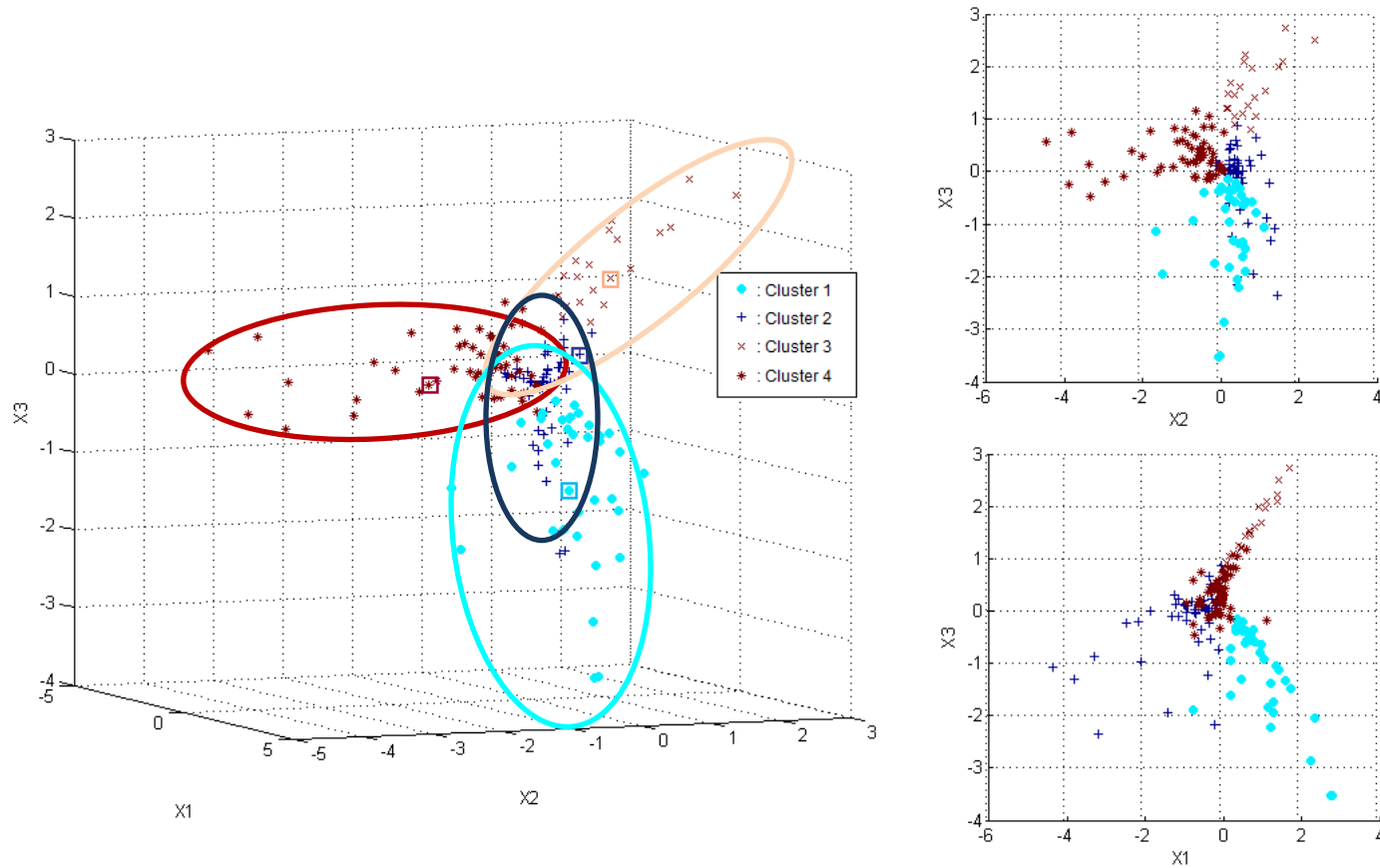
- Background on Locally Linear Embedding (LLE)
  - Data representation
  - Neighbourhood selection
  - Creating the manifold embedding
- Pre-operative reconstruction of an articulated 3D spine
  - Model initialization
  - Regression functions for inverse mapping
- **Pathology classification from the low-dimensional manifold**
- Inference of the intra-operative spine geometry from CT
  - Manifold-based constraints ensuring geometrical consistency
  - Optimization of manifold parameters for direct model representation

# Manifold-based classification

- Classification of 170 pre-operative patients with main thoracic deformities using a non-linear manifold embedding
- Extracted sub-groups from the underlying manifold structure using an unsupervised clustering approach
- Understand the inherent distribution and determine classes of pathologies which appear from the low-dimensional space



# Clustered sub-groups from the manifold



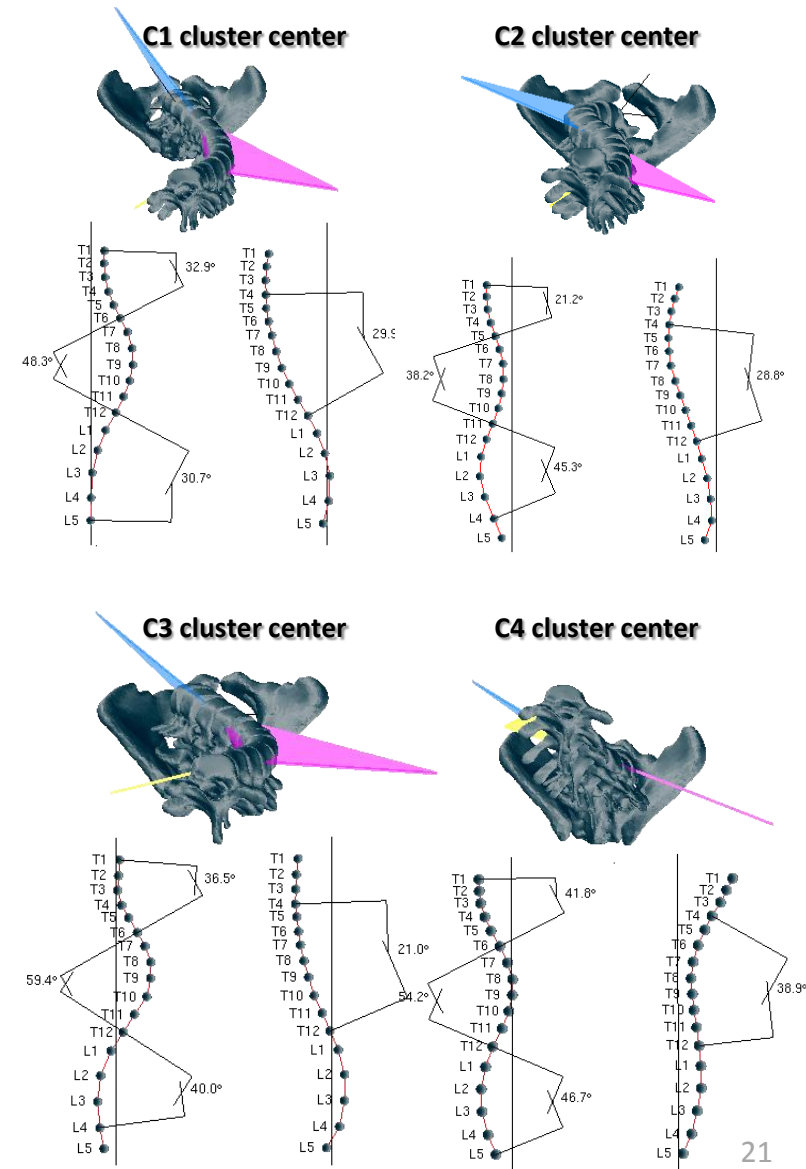
**Clustering of low-dimensional points**

Kadoury et al., Classification of three-dimensional thoracic deformities in adolescent idiopathic scoliosis from a multivariate analysis.

Eur. Spine J., 2011

# Clustered sub-groups from the manifold

Parameter	Cluster I (n = 37)	Cluster II (n = 55)	Cluster III (n = 21)	Cluster IV (n = 57)
Coronal Main Thoracic (MT) Cobb angle (°)	53 ± 11	39 ± 9	45 ± 14	45 ± 9
Kyphosis (°)	31 ± 15	26 ± 12	19 ± 12	39 ± 12
Lordosis (°)	-39 ± 12	-32 ± 15	-38 ± 12	-33 ± 12
MT plane of maximum curvature (PMC) rotation (°)	61 ± 30	71 ± 31	45 ± 24	53 ± 25
MT apical axial rotation (°)	-23 ± 11	-11 ± 8	-16 ± 8	-22 ± 8



Kadoury et al., Classification of three-dimensional thoracic deformities in adolescent idiopathic scoliosis from a multivariate analysis.

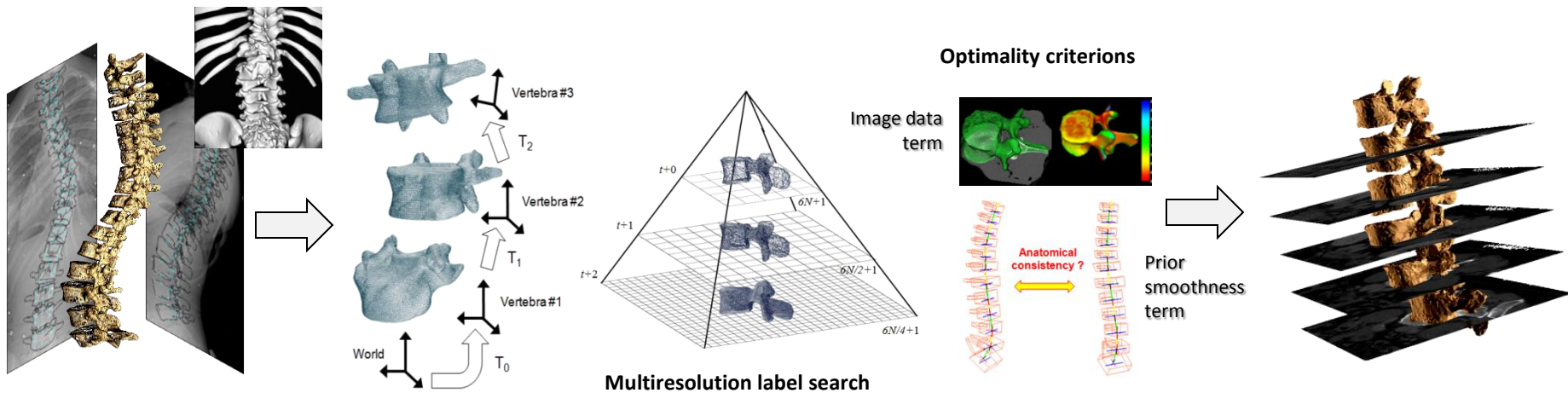
Eur. Spine J., 2011

# Outline

- Background on Locally Linear Embedding (LLE)
  - Data representation
  - Neighbourhood selection
  - Creating the manifold embedding
- Pre-operative reconstruction of an articulated 3D spine
  - Model initialization
  - Regression functions for inverse mapping
- Pathology classification from the low-dimensional manifold
- **Inference of the intra-operative spine geometry from CT**
  - Manifold-based constraints ensuring geometrical consistency
  - Optimization of manifold parameters for direct model representation

# Workflow for articulated 3D spine inference

- The pre-operative 3D spine model is inferred to procedural CT data acquired for corrective spine surgery

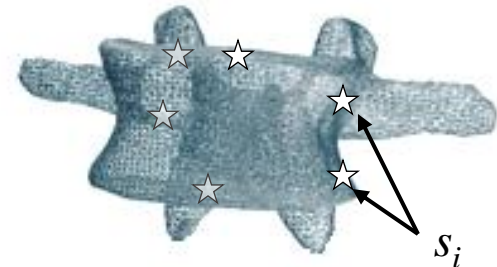


- The articulated spine model is optimized through a Markov Random Field (MRF) graph in order to achieve multi-modal registration.
- We propose an approach which avoids CT image segmentation, is computational efficient and solves the standing to lying pose deformation.

# Articulated deformable model (ADM) representation

- The spine model  $\mathbf{S} = [s_1, \dots, s_L]$  consists of an interconnection of  $L$  vertebrae  $s_i$  composed of:

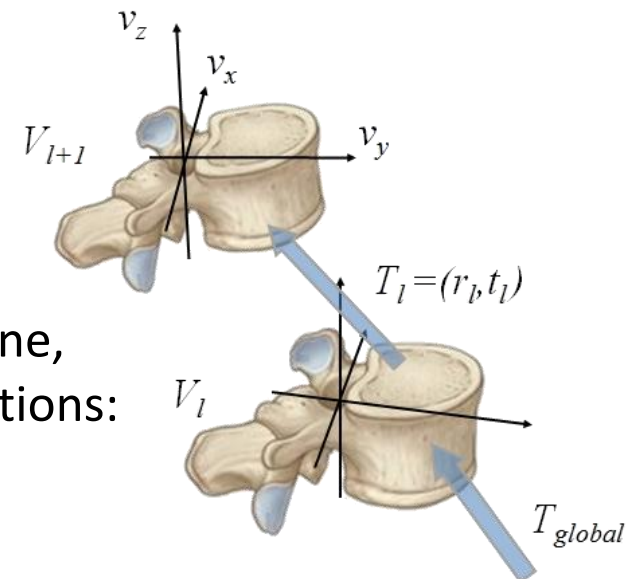
- The 3D landmarks  $s_i$  are used to rigidly register each vertebra to its upper neighbour.
- Triangular meshes with vertices  $\{v_i^j \mid j = 1, \dots, V\}$ , where the  $j^{\text{th}}$  vertex corresponds to approximately the same location for every shape  $i$ .



- The ADM is represented by a vector of local inter-vertebral rigid transformations modeled by  $T = \{R, t\}$  such that:  $A = [T_1, T_2, \dots, T_N]$

- To perform global anatomical modeling of the spine, we convert  $A$  to an absolute vector of transformations:

$$\mathbf{A}_{\text{abs}} = [T_1, T_1 \circ T_2, \dots, T_1 \circ T_2 \circ \dots \circ T_N]$$



# Transformation inference from higher order MRFs

- A successful inference between  $\mathbf{S}^0$  controlled by the articulations ( $\mathbf{A}_{\text{abs}}$ ) and the image  $I$  must be accomplished by establishing similarity criterions which will drive the model deformation towards the optimal solution.
- **Objective:** determine optimal displacement vectors  $\mathbf{D} = \{ \vec{d}_1, \dots, \vec{d}_n \}$  applied to the articulation  $T$  that give a good compromise between the encoded prior constraints established by manifold statistics and the fidelity to the image information:

$$(\vec{d}_1, \dots, \vec{d}_n) = \underset{\vec{d}_i}{\operatorname{argmin}} E(\mathbf{S}^0, I, (\vec{d}_1, \dots, \vec{d}_n))$$

- In turn, the energy function  $E$  can be decomposed into three costs related to the displacement vectors  $\vec{D} = \{ \vec{d}_1, \dots, \vec{d}_n \}$  in the transformation space :

$$E(\mathbf{S}^0, I, \vec{D}) = V(\mathbf{A}_{\text{abs}}^0 + \vec{D}, I) + V(\mathbf{N}, \vec{D}) + V(\mathbf{H}, \vec{D})$$

# Singleton and pairwise potential terms

- A data-related term  $V(\mathbf{A}_{\text{abs}}^0 + D, I)$  expressing the image cost and a local prior term  $V(\mathbf{N}, D)$  measuring deformation between neighboring vertebrae are integrated in  $E$ :

$$E = \sum_{i \in G} V_i(T_i^0 + \vec{d}_i, I)$$

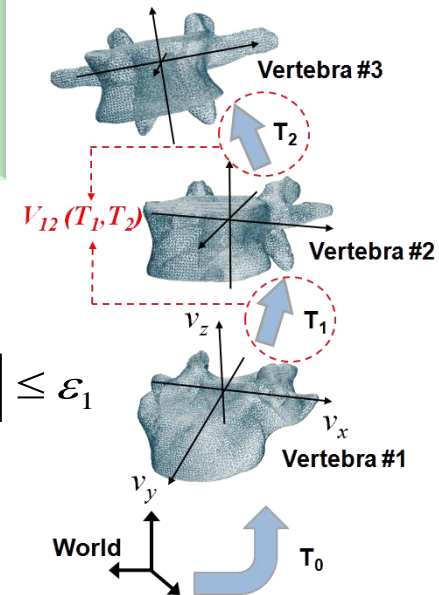
$$+ \lambda_{ij} \sum_{i \in G} \sum_{j \in N(i)} V_{ij}(T_i^0 + \vec{d}_i, T_j^0 + \vec{d}_j)$$

**Singleton potentials:** measures the support from the data (ex: image-based) without segmentation

$$\sum_{i \in G} V_i(T_i^0 + \vec{d}_i, I) = \int_{\Omega} \eta_x(I, S_i(T_i^0 + \vec{d}_i)) dT$$

**Pairwise constraints:** geometrical vertebral dependencies (smoothness term)

$$V_{ij}(0,1) = \begin{cases} |(T_i^0 + \vec{d}_i) - (T_j^0 + \vec{d}_j)| \leq \varepsilon_1 \\ \|\vec{d}_i\| - \|\vec{d}_j\| \leq \varepsilon_2 \end{cases}$$

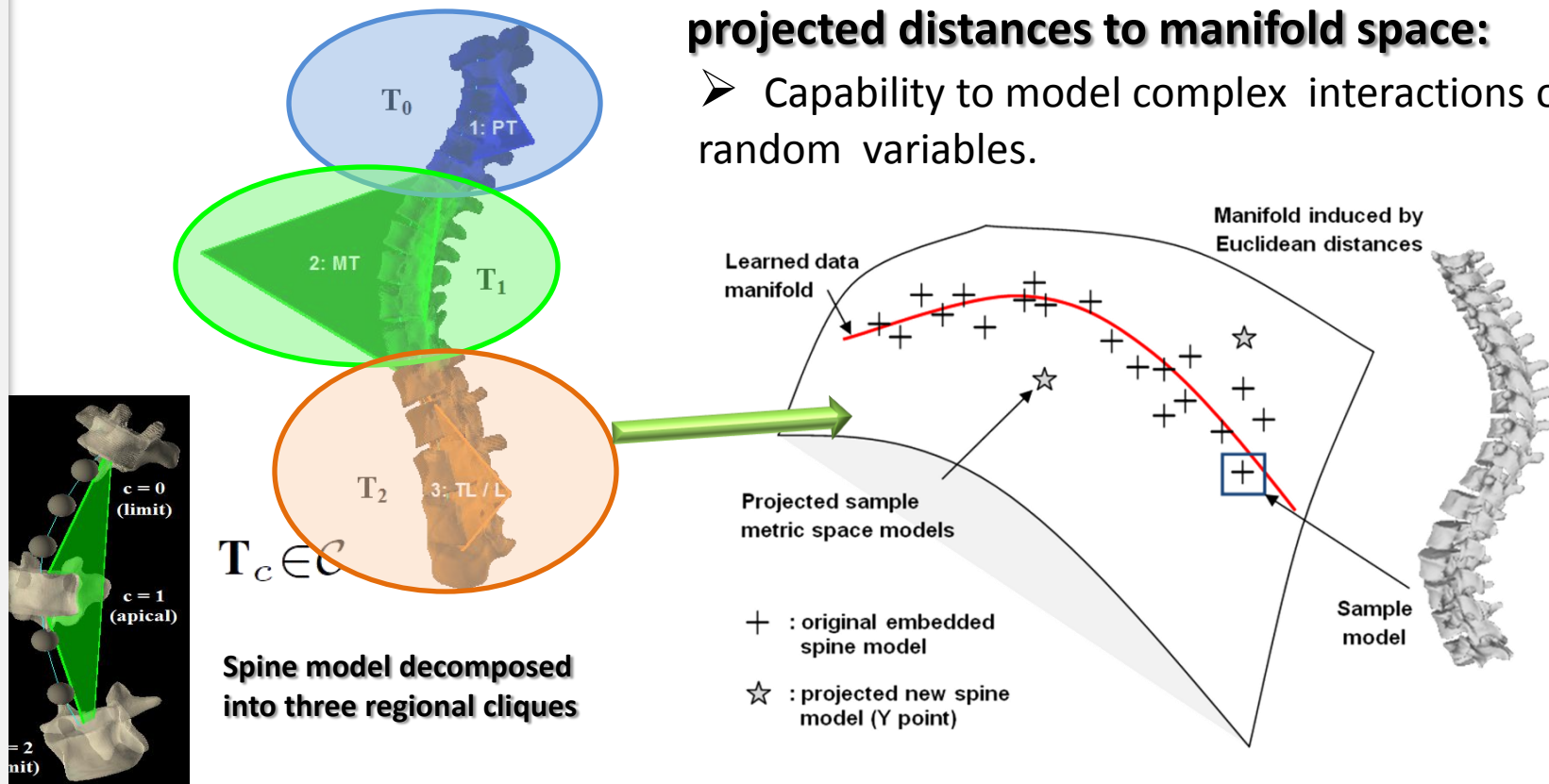


# Higher order clique potentials

- Most energy minimization based methods for solving computer vision problems assume the energy can be represented in terms of unary and pairwise potentials.

## Higher order clique variables encoded as projected distances to manifold space:

- Capability to model complex interactions of random variables.



# Manifold-constrained parameterization

- Potentials are parameterized with clique variables  $\mathbf{T}_c$  taking on corresponding costs  $\theta_q$  if the cliques are assigned to the displacement vectors  $d_c$ :

$$V_c(\mathbf{T}_c^0) = \min\left\{ \min_{q \in \{1, 2, \dots, t\}} \theta_q + \Delta_q(\mathbf{T}_c^0), \theta_{\max} \right\}$$

Cost-assigning function

- Costs  $\theta_q$  are manifold-defined geodesic distances evaluating the projection of clique variable to the prior distribution  $M$ :

$$E = \sum_{i \in G} V_i(T_i^0 + \vec{d}_i, I) + \lambda_{ij} \sum_{i \in G} \sum_{j \in N(i)} V_{ij}(T_i^0 + \vec{d}_i, T_j^0 + \vec{d}_j)$$

$$\theta_q = \left\| \psi(\mathbf{T}_c) - \Pi_{\phi(M)}(\psi(\mathbf{T}_c)) \right\|_F$$

Low-dimensional clique representation

Projection onto manifold space  $M$

**High order constraints:**  
global geometrical dependencies for a group of vertebrae

# Point-based comparison

- Anatomical landmark deviations from “bronze-standard” are compared with pairwise cost functions.
- Evaluation on 20 patients with low to moderate deformations.

	Image + pairwise terms (MICCAI 2009)		
Region	Mean (mm)	RMS (mm)	Max (mm)
Thoracic vertebrae	2.01	<b>2.25</b>	5.26
Lumbar vertebrae	1.55	<b>1.98</b>	4.81
<b>Total vertebrae</b>	1.87	<b>2.12</b>	5.08

	Higher order method		
Region	Mean (mm)	RMS (mm)	Max (mm)
Thoracic vertebrae	1.54	<b>1.73</b>	4.64
Lumbar vertebrae	2.18	<b>2.06</b>	4.14
<b>Total vertebrae</b>	1.70	<b>1.85</b>	4.49

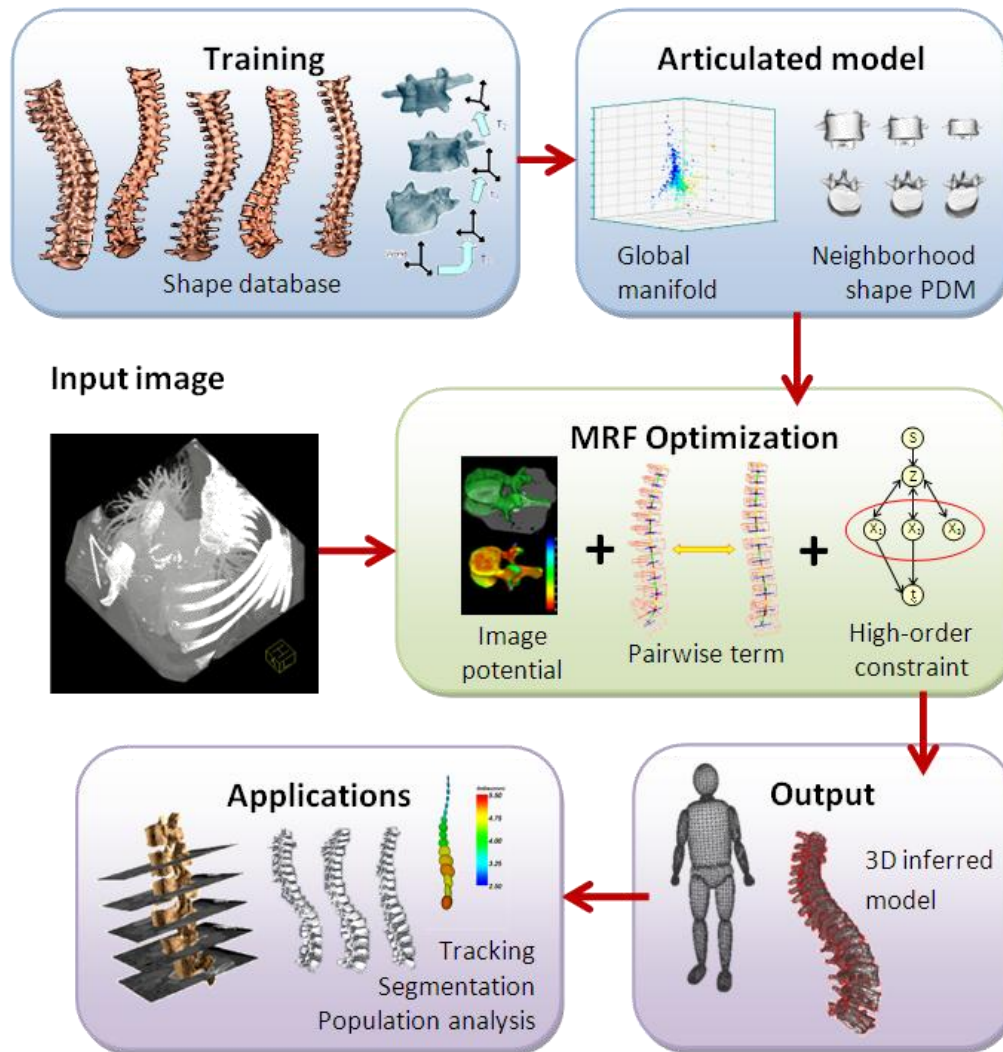


Initial alignment



High order MRF inference

# 3D inference of articulated spine models from the manifold embedding



- Inference with respect to the manifold and shape parameters is performed using a High-order Markov Random Field (HOMRF).
- Captures the statistical distribution of the underlying manifold and respects image support in the spatial domain

Kadoury et al., Nonlinear Embedding towards Articulated Spine Shape Inference using Higher-Order MRFs. MICCAI, 2010.

# Nearest neighbour selection

- Estimates the distance of articulated models  $i, j$  based on their representation as feature vectors  $\mathbf{A}_{\text{abs}}^i$  and  $\mathbf{A}_{\text{abs}}^j$ .
- Allowing to discern between articulated shape deformations in a topological invariant framework.

$$d_M(\mathbf{A}_{\text{abs}}^i, \mathbf{A}_{\text{abs}}^j) = \sum_{k=1}^L \|c_k^i - c_k^j\| + d_G(R_k^i, R_k^j)$$

- Evaluates the intrinsic distances in the L2 norm and defines diffeomorphism between rotation neighborhoods in  $M$  using geodesics.
- Rotational distances are computed with the following norm:

$$d_G(R_k^i, R_k^j) = \left\| \log((R_k^i)^{-1} R_k^j) \right\|_F$$

based on the geodesic distances ( $d_G$ ) in the 3D manifold.

# Ambient space mapping

**Forward-inverse mapping** used to obtain the articulation vector for a new embedded point in the ambient space.

- Theoretically the manifold should follow the conditional expectation which captures the regional trend of the data in  $D$ -space:

$$f(Y_i) \equiv E(\mathbf{A}_{\text{abs}}^i \mid M(A_i) = Y_i) = \int A_i \frac{p(Y_i, A_i)}{p_{M(A_i)}(Y_i)} dD$$

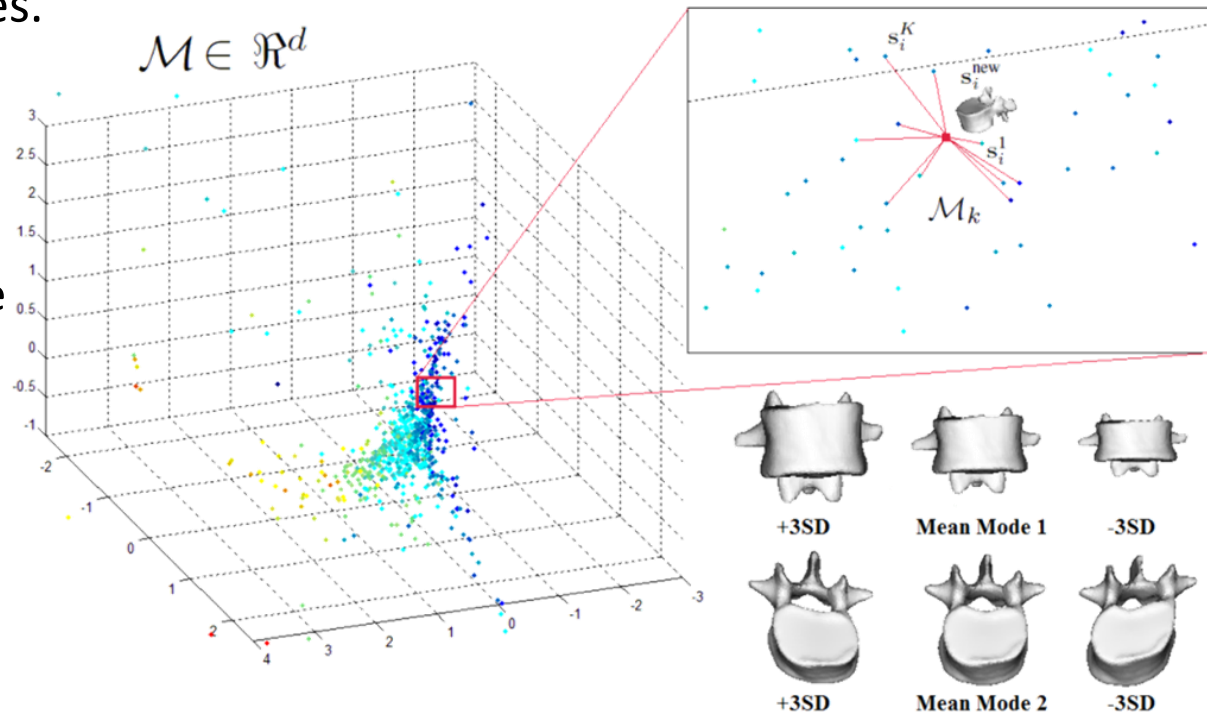
- Based on *Nadaraya-Watson* regression:
  - Estimates the relationship between the  $D$ -space and manifold  $M$  data points as a joint distribution;
  - Constrains the regression for similar data points in a local vicinity with Gaussian kernels.

$$f_{NW}(Y_i) = \arg \min_{\mathbf{A}_{\text{abs}}^i} \frac{\sum_{j \in N(i)} G(Y_i, Y_j) d_M(\mathbf{A}_{\text{abs}}^i, \mathbf{A}_{\text{abs}}^j)}{\sum_{j \in N(i)} G(Y_i, Y_j)}$$

# Local shape appearances

- Capturing local object appearance lies on the assumption that global models, represented in a local neighborhood of  $M$ , will also manifest similar local geometries.

- Given a data point  $Y_j$  and its  $K$  neighbors, the local shape model  $s_i$ , representing the  $i^{\text{th}}$  element of the ADM, is obtained by building a particular class of shapes  $\{s_i^1, \dots, s_i^K\}$ .



# Inference through MRF optimization

- Inference with respect to image and manifold parameters is performed as a high order MRF optimization.
- Optimal embedded manifold point  $Y = (\mathbf{y}_1, \dots, \mathbf{y}_d)$  represents the **global** spine model and **individual** shape variation is described by the weight vector  $W = (\mathbf{w}_1, \dots, \mathbf{w}_n)$  in a localized sub-patch:

$$(\{\mathbf{y}_1, \dots, \mathbf{y}_d\}; \{\mathbf{w}_1, \dots, \mathbf{w}_n\}) = \arg \min_{\delta, \omega} E(\mathbf{S}^0, I, \Delta, \Omega)$$

- Energy function  $E$  involves:

- 1 Data-related term expressing image cost.
- 2 Global prior term measuring support in manifold space.
- 3 Clique variables referring to local shape constellations.

$$E(\mathbf{S}^0, I, \Delta, \Omega) = V(\mathbf{Y}^0 + \Delta, I) + \alpha V(\mathbf{N}, \Delta) + \beta V(\mathbf{H}, \Delta, \Omega)$$

1

2

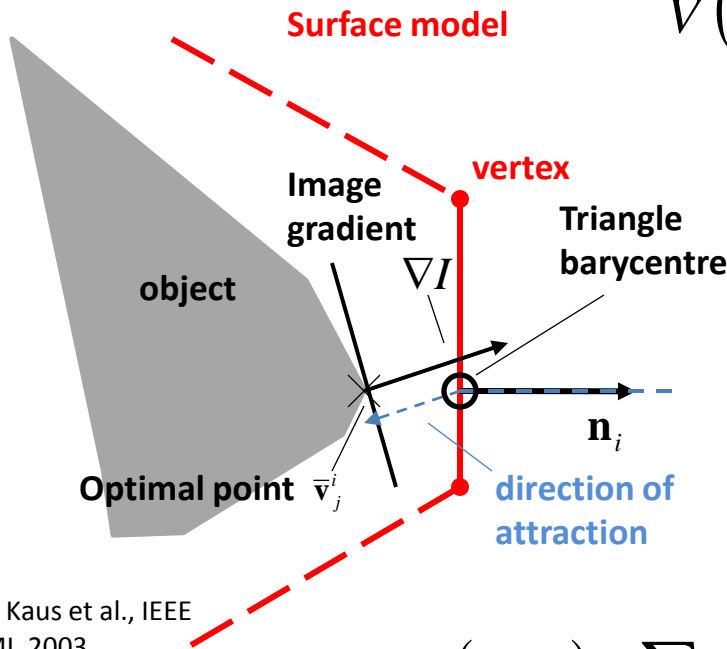
3

# Global alignment of the ADM

- Image-related term  $V(\mathbf{Y}^0 + \Delta, I)$  (unary potentials) attracts each  $L$  mesh object of the ADM to the highest gradient potential:

$$V(\mathbf{Y}^0 + \Delta, I) = V(f_{\text{NW}}(\{y_1 + \delta_1, \dots, y_d + \delta_d\}), I)$$

$$= V(\mathbf{A}_{\text{abs}}^0 + \vec{D}, I) = \sum_{i=1}^L V_i(s_i * (T_i^0 + d_i), I)$$

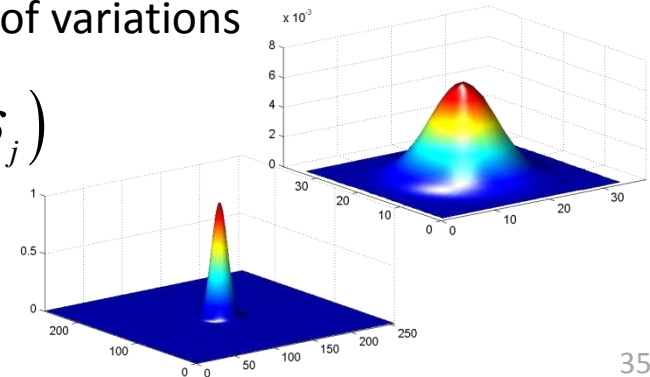


$$V_i(\mathbf{s}, I) = - \sum_{\mathbf{v}_j \in \mathbf{s}} \mathbf{n}_i^T(\mathbf{v}_j) \nabla I(\mathbf{v}_j)$$

- Pairwise potentials  $V(\mathbf{N}, \Delta)$  (anatomical smoothness) ensure that the deformations applied to point coordinates is regular in the non-linear vicinity of variations

$$V(\mathbf{N}, \Delta) = \sum_{i \in G} \sum_{j \in N(i)} V_{ij}(y_i^0 + \delta_i, y_j^0 + \delta_j)$$

$$\Rightarrow V_{ij} = P(\| (y_i^0 + \delta_i) - (y_j^0 + \delta_j) \|, N(i))$$



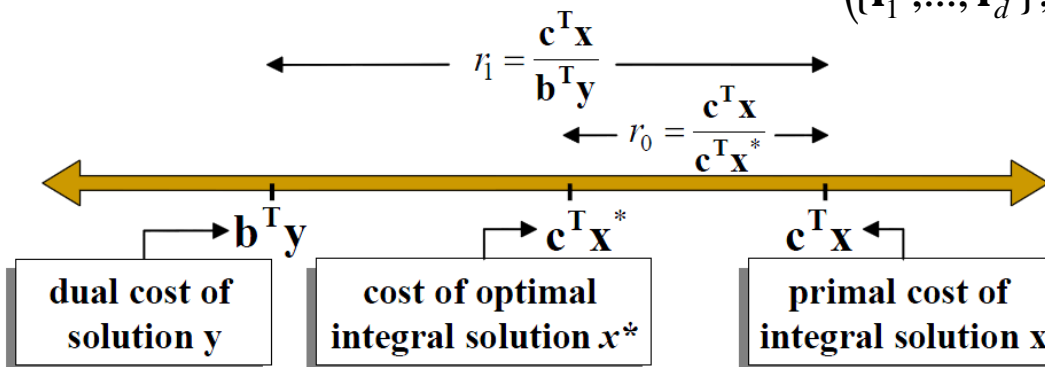
# Energy minimization

- Optimization strategy of the energy term in the continuous domain:
  - Convexity of the solution domain is not guaranteed.
  - Prone to non-linearity and local minimums.

$$\begin{aligned}
 E(\mathbf{S}^0, I, \bar{\Delta}, \Omega) &= V(f_{\text{NW}}(\{y_1 + \bar{\delta}_1, \dots, y_d + \bar{\delta}_d\}), I) \\
 &+ \alpha \sum_{i \in G} \sum_{j \in N(i)} V_{ij}(y_i^0 + \bar{\delta}_i, y_j^0 + \bar{\delta}_j) \\
 &+ \beta \sum_{c \in C} V_c(\mathbf{w}_c^0 + \omega_c)
 \end{aligned}$$

- Adopt a discrete optimization approach guaranteeing the global optimum

$$(\{\mathbf{l}_1^{\bar{\Delta}}, \dots, \mathbf{l}_d^{\bar{\Delta}}\}; \{\mathbf{l}_1^{\Omega}, \dots, \mathbf{l}_n^{\Omega}\}) = \arg \min_{\mathbf{l}_1^{\bar{\Delta}}, \mathbf{l}_1^{\Omega} \in L^{\bar{\Delta}}, L^{\Omega}} E(\mathbf{S}^0, I, L^{\bar{\Delta}}, L^{\Omega})$$

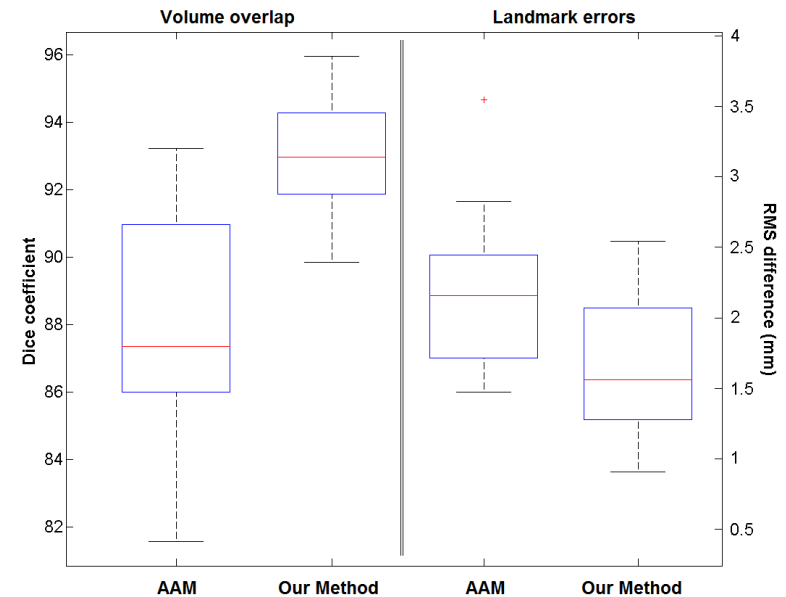
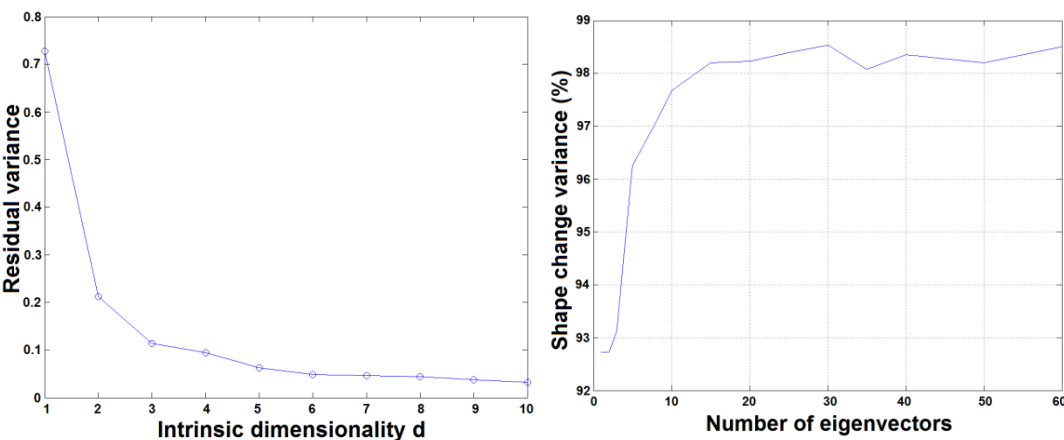
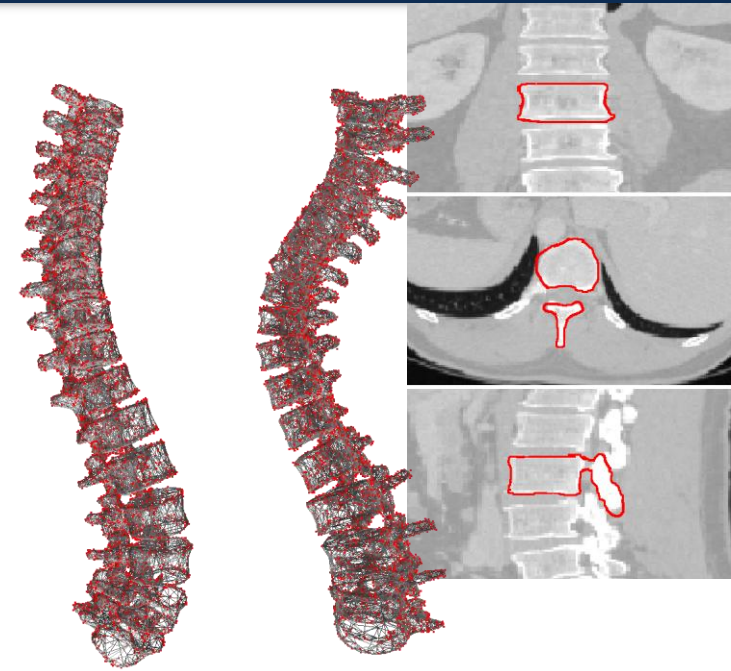


Inference problem is solved in a discrete domain by applying duality theory in linear programming.

N. Komodakis, et al. CVIU, 112(1):14–29, 2008

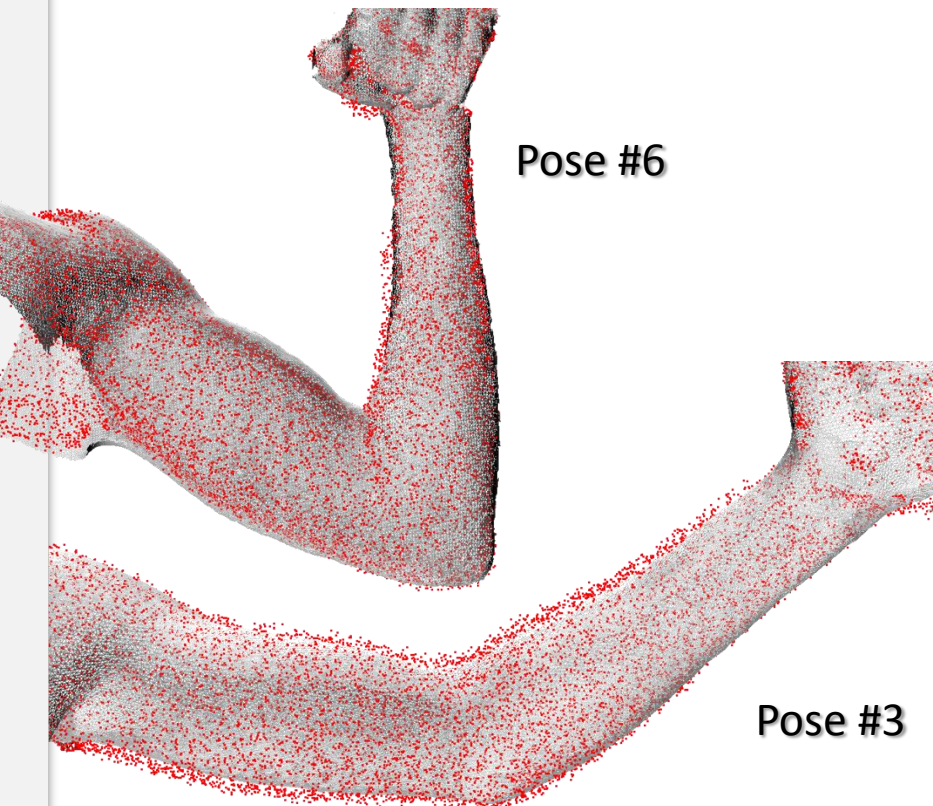
# Experimental results

- Modeling pathological spinal columns represented as articulated shapes for CT inference.
  - Training on 711 models exhibiting varying types of deformities.
  - Meshes composed between 3831 and 6942 vertices.
  - Evaluation on 20 pathological cases.



# Experiments on articulated arm poses

- Arm-pose estimation from sparse scan range data acquisitions (GRAIL, Univ. Wash.) ( $d = 5$ ,  $n = 5$ ,  $K = 8$ )
- 7 arm poses were tested with comparison to ground-truth and shape completion method<sup>7</sup>



Pose	SCAPE-like [2]		Proposed method	
	Land.(mm)	Surf.	Land.(mm)	Surf.
#1	$3.6 \pm 1.7$	8.4	$2.1 \pm 0.8$	4.3
#2	$4.4 \pm 1.4$	8.6	$1.5 \pm 1.0$	4.0
#3	$6.8 \pm 2.9$	10.5	$4.1 \pm 2.5$	5.5
#4	$5.3 \pm 3.3$	9.1	$3.4 \pm 1.0$	6.1
#5	$4.5 \pm 2.3$	8.7	$4.6 \pm 2.9$	3.2
#6	$7.1 \pm 3.5$	11.2	$2.9 \pm 0.8$	4.3
#7	$3.0 \pm 1.6$	6.9	$1.2 \pm 0.5$	2.6

<sup>7</sup>D. Anguelov et al. SCAPE: Shape Completion and Animation of People. In SIGGRAPH, pages 408–416, 2005

# Conclusions

- Shape analysis of articulated models is a challenging problem due to the difficulty in constraining the higher number of transformation variables.
- Modeling complex, non-linear patterns of prior deformations in a Riemannian manifold embedding.
- Offers the possibility to learn the variations of spinal shape in complex corrective procedures.
- Whole spine body deformation is achieved by means of novel high order cliques in the optimization to impose global shape constraints.
- General applicability to discriminate between normal and pathological cases in other organs/modalities.



# *Thank you*

**Sponsoring parties:**

*Inria*  
INVENTEURS DU MONDE NUMÉRIQUE

Fonds de recherche  
sur la nature  
et les technologies

Québec



**biospace med**

**Acknowledgments:**

Nikos Paragios

Dr. Hubert Labelle

Philippe Labelle